ARTICLE

BIOTECHNOLOGY and BIOENGINEERING

Physiological and Transcriptional Characterization of *Escherichia Coli* Strains Lacking Interconversion of Phosphoenolpyruvate and Pyruvate When Glucose and Acetate are Coutilized

Andrea Sabido,[1] Juan Carlos Sigala,[2] Georgina Hernández-Chávez,[1] Noemí Flores,[1] Guillermo Gosset,[1] Francisco Bolívar[1]

[1]Departamento de Ingeniería Celular y Biocatálisis, Instituto de Biotecnología, Universidad Nacional Autónoma de México, Cuernavaca, Mor., México

[2]Departamento de Procesos y Tecnología, Universidad Autónoma Metropolitana-Cuajimalpa, Av. Vasco de Quiroga 4871, Col. Santa Fe, Del. Cuajimalpa. CP 05348, D. F. México; telephone: +52-55-26-36-38-00 ext. 3854; fax: +52-55-26-36-38-00 ext. 3854; e-mail: jsigala@correo.cua.uam.mx

ABSTRACT: Phosphoenolpyruvate (PEP) is a precursor involved in the biosynthesis of aromatics and other valuable compounds in *Escherichia coli*. The PEP:carbohydrate phosphotransferase system (PTS) is the major glucose transport system and the largest PEP consumer. To increase intracellular PEP availability for aromatics production purposes, mutant strains of *E. coli* JM101 devoid of the *ptsHIcrr* operon (PB11 strain) have been previously generated. In this derivative, transport and growth rate on glucose decreased significantly. A laboratory evolved strain derived from PB11 that partially recovered its growth capacity on glucose was named PB12. In the present study, we blocked carbon skeletons interchange between PEP and pyruvate (PYR) in these *ptsHIcrr*$^-$ strains by deleting the *pykA*, *pykF*, and *ppsA* genes. The PB11 *pykAF*$^-$ *ppsA*$^-$ strain exhibited no growth on glucose or acetate alone, but it was viable when both substrates were consumed simultaneously. In contrast, the PB12 *pykAF*$^-$ *ppsA*$^-$ strain displayed a low growth rate on glucose or acetate alone, but in the mixture, growth was significantly improved. RT-qPCR expression analysis of PB11 *pykAF*$^-$ *ppsA*$^-$ growing with both carbon sources showed a downregulation of all central metabolic pathways compared with its parental PB11 strain. Under the same conditions, transcription of most of the genes in PB12 *pykAF*$^-$ *ppsA*$^-$ did not change, and few like *aceBAK*, *sfcA*, and *poxB* were overexpressed compared with PB12. We explored the aromatics production capabilities of both *ptsHIcrr*$^-$ *pykAF*$^-$ *ppsA*$^-$ strains and the engineered PB12 *pykAF*$^-$ *ppsA*$^-$ *tyrR*$^-$ *pheA*$^{ev2+}$/pJLB*aroG*^{fbr}*tktA* enhanced the yield of aromatic compounds when coutilizing glucose and acetate compared with the control strain PB12 *tyrR*$^-$ *pheA*$^{ev2+}$/pJLB*aroG*^{fbr}*tktA*. Biotechnol. Bioeng. 2014;111: 1150–1160.

KEYWORDS: PTS system; PEP–PYR node; glucose and acetate coutilization; aromatic compounds

Correspondence to. J.C. Sigala
Contract grant sponsor: CONACyT
Contract grant number: 105782
Contract grant sponsor: FONSEC/SSA/ISSSTE/CONACyT
Contract grant number: 44126
Contract grant sponsor: DGAPA-PAPIIT-UNAM
Contract grant number: IN205811
Received 16 August 2013; Revision received 5 December 2013; Accepted 18 December 2013
Accepted manuscript online 28 December 2013;
Article first published online 28 January 2014 in Wiley Online Library (http://onlinelibrary.wiley.com/doi/10.1002/bit.25177/abstract).
DOI 10.1002/bit.25177

Introduction

The phosphoenolpyruvate–pyruvate–oxaloacetate (PEP–PYR–OAA) node involves a set of reactions that interconnect the main pathways of central carbon metabolism (Fig. 1a), and thus, it is responsible for the distribution of carbon flux among catabolism, anabolism and energy supply for the cell. In *E. coli*, some of the enzymes that have been implicated in this node are as follows: PEP carboxylase (Ppc), PYR kinases A and F (PykA and F), PEP carboxykinase A (PckA), PEP synthetase A (PpsA), malic enzymes (MaeB and SfcA), and the PTS system (Sauer and Eikmanns, 2005). Several approaches, such as their in vivo metabolic fluxes and the relevance of flux redirection on cell physiology have been used to study the function of the enzymes involved in the node (Emmerling et al., 2002; Fischer and Sauer, 2003; Siddiquee et al., 2004a,b; Yang et al., 2003). The interest in this node arises from the need to manipulate PEP availability.

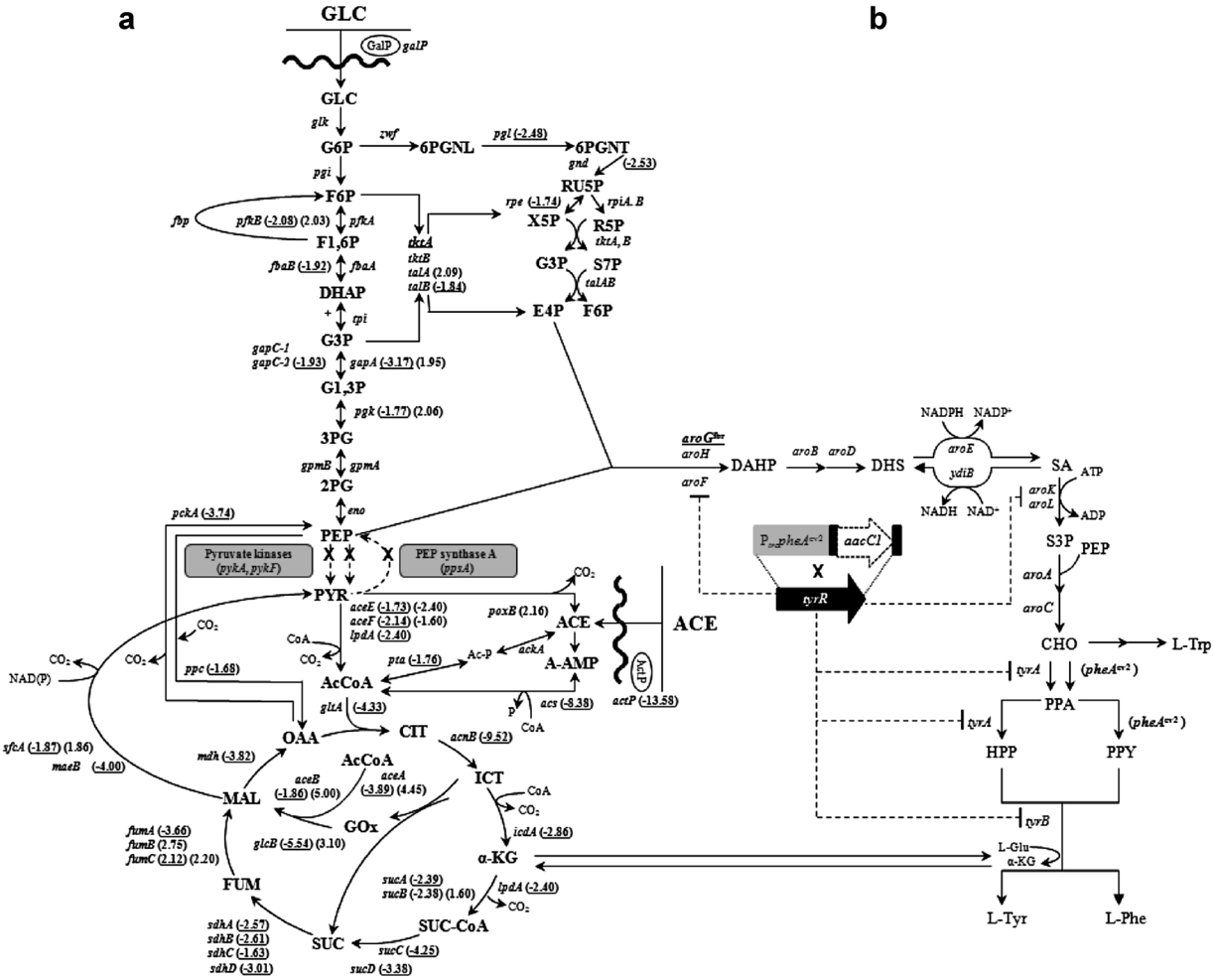

Figure 1. Central metabolic routes and the aromatic compounds biosynthesis showing key metabolites and the genes involved in their transformation. (**a**) Central carbon metabolism showing RT-qPCR values of upregulated genes (1.6-fold or higher) or downregulated genes (−1.6-fold or lower) in parentheses for the strain PB12 *pykAF*$^{-}$ *ppsA*$^{-}$ and underlined in parentheses for strain PB11 *pykAF*$^{-}$ *ppsA*$^{-}$. Reactions and deleted genes from the PEP–PYR node are indicated with discontinuous arrows and highlighted in boxes respectively. The RT-qPCR values of all the genes are presented in Table III. The abbreviations are as follows: glucose (GLC), glucose-6-phosphate (G6P), fructose-6-phosphate (F6P), fructose-1,6-phosphate (F1,6P), dihydroxyacetone phosphate (DHAP), glyceraldehyde-3-phosphate (G3P), glyceraldehyde-1,3-phosphate (G1,3P), 3-phosphoglycerate (3PG), 2-phosphoglycerate (2PG), phosphoenolpyruvate (PEP), pyruvate (PYR), acetate (Ace), acetyl-CoA (AcCoA), acetyl-phosphate (Ac-P), acetyl-AMP (A-AMP), citrate (CIT), isocitrate (ICT), glyoxylate (GOx), α-ketoglutarate (α-KG), succinyl-coenzyme A (SUC-CoA), succinate (SUC), fumarate (FUM), malate (MAL), oxaloacetate (OAA), 6-phosphogluconolactone (6PGNL), 6-phosphogluconate (6PGNT), ribulose-5-phosphate (RU5P), ribose-5-phosphate (R5P), xylulose-5-phosphate (X5P), seudoheptulose-7-phosphate (S7P), erythrose-4-phosphate (E4P), and 3-deoxy-D-arabino-heptulosonate-7-phosphate (DAHP); (**b**) the common aromatic pathway leading to L-Phe, L-Tyr, and L-Trp and other compounds. Genetic modifications performed in this study are shown with plasmid-expressed genes underlined, chromosomal integrated genes in parentheses and inactivated genes with a cross (details in Materials and Methods and Supplementary file 1). Consecutive arrows indicate more than one catalytic step. The abbreviations are as follows: 3-dehydroshikimic acid (DHS), shikimic acid (SA), shikimate 3-phosphate (S3P), chorismate (CHO), L-tryptophan (L-Trp), prephenate (PPA), 4-hydroxyphenylpyruvate (HPP), phenylpyruvate (PPY), L-tyrosine (L-Tyr), L-phenylalanine (L-Phe), and L-Glutamate (L-Glu).

As a phosphate donor, PEP is involved in glucose uptake by the PTS system in various bacteria including *E. coli* (Postma et al., 1996). This metabolite is also a building block for the production of the aromatic amino acids and their derived compounds. The PTS system is the largest consumer of PEP, followed by PYR kinases and Ppc, and leaves only a small fraction of carbon flux for the synthesis of aromatic compounds (Flores et al., 2002; Holms, 1986). In this regard, our group has generated *E. coli* mutants devoid of PTS by deleting the *ptsHIcrr* operon (PB11 strain), a strategy that, in theory, may double PEP availability. However, glucose transport and growth rates in these *ptsHIcrr*$^{-}$ mutants decreased significantly. To overcome this limitation, an adaptive evolution process was performed to obtain a strain derived from PB11 termed PB12 (Flores et al., 2005, 2007), which partially recovered its growth capacity on glucose. As a result of this process, several point mutations and a 10,328 bp chromosomal deletion that removed the *rppH*, *mutH*, and *galR* genes were generated in PB12. It is proposed that simultaneous deletion of these three genes is mainly responsible for the faster growth rate of the PB12 strain on glucose compared with PB11 (Aguilar et al., 2012).

Transcriptome profiling by reverse transcriptase quantitative real-time PCR (RT-qPCR) in the *ptsHIcrr*$^{-}$ strains

growing on glucose, showed that the transcriptional levels of gluconeogenic genes are increased in PB11 compared with JM101. In contrast, the transcriptional levels of glycolytic genes are increased only in PB12 compared with JM101 and PB11 (Flores et al., 2005). A carbon flux analysis also demonstrated that PB12 increased its glycolytic flux, whereas PB11 reduced it compared with its parental strain, JM101 (Flores et al., 2002). It is important to note that the glycolytic and gluconeogenic pathways function simultaneously in these *ptsHIcrr*$^-$ strains, allowing the coutilization of secondary carbon sources in the presence of glucose due to the absence of the EIIA^{Glc} component, which is mainly responsible for catabolite repression (Flores et al., 2005; Martínez et al., 2008; Postma et al., 1996). When grown in acetate as carbon source, PB11 and PB12 have lower growth rates. It is proposed that due to diminished cAMP levels in these *ptsHIcrr*$^-$ strains, certain gluconeogenic genes such as *acs*, *actP*, *maeB*, and *pckA* are not properly induced on acetate (Sigala et al., 2009).

With the aim of understanding the changes in cellular physiology in response to knockout mutations in the PEP–PYR–OAA node, different strains lacking the *pykA*, *pykF*, or *ppc* genes have been generated (Covert and Palsson, 2002; Emmerling et al., 2002; Meza et al., 2012; Siddiquee et al., 2004a,b). Single and double mutants of gluconeogenic genes such as *pckA*, *ppsA*, *maeB*, and *sfcA* have also been studied (Oh et al., 2002; Yang et al., 2003). However, these approaches have been reviewed from two different perspectives: either the effects of these knockouts on the glycolytic metabolism or their effects on the TCA cycle during growth on single carbon substrates. Therefore, in the present work, we investigated the feasibility of blocking interconversion of PEP and PYR in strains devoid of the PTS system and with additional deletions in the *pykA*, *pykF*, and *ppsA* genes. We evaluated the viability of the generated derivatives on glucose, on acetate and during simultaneous utilization of both carbon sources. Acetate was selected as a gluconeogenic substrate since its catabolism in *E. coli* could activate properly the TCA cycle, the glyoxylate shunt and the anaplerotic reactions (malic and PckA enzymes) (Oh et al., 2002).

In addition, in the PB11 *pykAF*$^-$ *ppsA*$^-$ and PB12 *pykAF*$^-$ *ppsA*$^-$ strains, we determined the specific growth rate (μ), specific glucose plus acetate consumption rate (q_s) and biomass/substrate yield ($Y_{x/s}$) as well as the expression profiles of central carbon metabolism genes by RT-qPCR during coutilization of glucose and acetate. Finally, to determine the effects of the modifications at the PEP–PYR node on PEP availability, engineered derivatives of the *ptsHIcrr*$^-$ *pykAF*$^-$ *ppsA*$^-$ strains were generated and tested for aromatics production.

Materials and Methods

Bacterial Strains and Plasmids

E. coli strains and plasmids used in this study are presented in Table I.

Genetic Procedures and Recombinant DNA Techniques

Mutant strains of PB11 and PB12 with inactive *pykA*, *pykF*, and *ppsA* genes were constructed by inserting either a chloramphenicol (*cat*) gene flanked by two parallel *loxP* (Palmeros

Table I. *E. coli* strains and plasmids used in this study.

Strains	Relevant characteristics	References
PB11	JM101 Δ(*ptsH*, *ptsI*, *crr*)::*kan*	Messing (1979), Flores et al. (1996, 2005)
PB12	PB11 laboratory evolved strain with 23 non-synonymous and 16 synonymous point mutations and a chromosomal deletion that removed 12 genes, among them, the *rppH*, *mutH*, and *galR* genes	Flores et al. (1996, 2005), Aguilar et al. (2012)
PB11 *pykAF*$^-$ *ppsA*$^-$	PB11 *pykA*::*loxP*, *pykF*::*loxP*, *ppsA*::*frt-cat-frt*	This work
PB12 *pykAF*$^-$ *ppsA*$^-$	PB12 *pykA*::*loxP*, *pykF*::*loxP*, *ppsA*::*frt-cat-frt*	This work
PB11 *tyrR*$^-$ *pheA*$^{ev2+}$/pJLB*aroG*^{fbr}*tktA*	PB11 *tyrR*::*pheA*^{ev2}, *loxP*/pJLB*aroG*^{fbr}*tktA*	This work
PB12 *tyrR*$^-$ *pheA*$^{ev2+}$/pJLB*aroG*^{fbr}*tktA*	PB12 *tyrR*::*pheA*^{ev2}, *loxP*/pJLB*aroG*^{fbr}*tktA*	This work
PB11 *pykAF*$^-$ *ppsA*$^-$ *tyrR*$^-$ *pheA*$^{ev2+}$/pJLB*aroG*^{fbr}*tktA*	PB11 *pykA*::*loxP*, *pykF*::*loxP*, *ppsA*::*frt*, *tyrR*::*pheA*^{ev2}, *loxP*/pJLB*aroG*^{fbr}*tktA*	This work
PB12 *pykAF*$^-$ *ppsA*$^-$ *tyrR*$^-$ *pheA*$^{ev2+}$/pJLB*aroG*^{fbr}*tktA*	PB12 *pykA*::*loxP*, *pykF*::*loxP*, *ppsA*::*frt*, *tyrR*::*pheA*^{ev2}, *loxP*/pJLB*aroG*^{fbr}*tktA*	This work
Plasmids		
pJLB*aroG*^{fbr}*tktA*	*aroG*^{fbr} gene under control of the *lac*UV5 promoter and *tktA* under its native promoter; carries *lacI*^{q} and *tet* genes. Replication origin from pACYC184	Balderas-Hernández et al. (2009)
pLoxGen*trc*	Expression plasmid carrying the *trc* promoter, a multiple cloning site, the T1 and T2 *rrnB* terminator sequences, the *lacI*^{q} and *loxP*-flanked *aacC1* resistance genes. Replication origin from pBR322.	Sabido et al. (2013)
pLoxGen*trcpheA*^{ev2}	Derivative of pLoxGen*trc* carrying the *pheA*^{ev2} gene	This work
pTrc*pheA*^{ev2}	Evolved *pheA* gene under the control of the lacUV5 promoter. Ev^2 means 2nd version of evolved *pheA*^{fbr} gene	Báez-Viveros et al., (2004)

et al., 2000) or *frt* sites. The PCR products of the disrupted genes were used to generate the corresponding mutants following the method published by Datsenko and Wanner (2000).

For aromatic amino acids production, one copy of the gene coding for an evolved mutant version of the chorismate mutase–prephenate dehydratase (PheA) enzyme, under control of the P_{trc} promoter, was integrated into the TyrR chromosomal locus of strains PB11, PB12, and their *pykAF*$^-$ *ppsA*$^-$ derivatives (details in Supplementary file 1). The simultaneous integration of the *pheA*^{ev2} gene and the parallel interruption of the native *tyrR* gene was performed with the goal of redirecting carbon flux towards the synthesis of both L-Phe and L-Tyr aromatic amino acids (Fig. 1b).

The resulting strains were transformed with plasmid pJLB*aroG*^{fbr}*tktA*, which harbors the *aroG*^{fbr} gene encoding a feedback inhibition resistant mutant of DAHP synthase. It also contains the *tktA* gene in order to avoid a limitation for E4P (Balderas-Hernández et al., 2009; Escalante et al., 2010). All primers used in this study are listed in Supplementary file 2.

Growth Media and Cultivation Conditions

For flask cultures, M9 mineral medium containing 6 g/L Na_2HPO_4, 0.5 g/L NaCl, 3 g/L KH_2HPO_4, 1 g/L NH_4Cl, 240.9 mg/mL $MgSO_4$, 11.1 mg/L $CaCl_2$, 2.0 mg/L vitamin B1, and 2 g/L glucose, 3 g/L acetate, or 2 g/L glucose plus 3 g/L acetate was used. Inoculum started from frozen vials stored at −72°C on glycerol, inoculated on LB medium overnight at 37°C and then cultured in M9 medium with glucose (2 g/L), acetate (3 g/L), or a mixture of glucose (2 g/L) plus acetate (3 g/L). When cultures reached exponential growth phase, they were inoculated into the same prewarmed, fresh medium under the same substrate conditions at an initial optical density at 600 nm (OD_{600nm}) of 0.1. All cultures were performed in duplicates thrice.

Cell samples for RNA isolation were collected in log phase at $OD_{600nm} = 1$ from 1 L fermentors containing 750 mL of M9 medium with 2 g/L glucose plus 3 g/L acetate as carbon sources, at 37°C, 600 rpm, pH controlled at 7 with NH_4OH (2.8–3.0%) and an air flow rate of 1 vvm, starting at an $OD_{600nm} = 0.1$ (Flores et al., 2005).

Resting Cells

The total aromatic compounds (TAC) production, specific rates (q_{TAC}), and yields ($Y_{TAC/Glc+Ace}$) were determined during resting cells experiments (calculations in Supplementary file 1). M9 medium with glucose (4 g/L) plus acetate (6 g/L), and yeast extract (2 g/L) was utilized for growing the inocula in resting cells experiments. Inocula were washed once with M9 medium and resuspended in 50 mL of the same medium with glucose (2 g/L) and acetate (3g/L) as starting concentrations in 250 mL baffled flasks, lacking yeast extract. For the PB12 *tyrR*$^-$ *pheA*$^{ev2+}$/pJLB*aroG*^{fbr}*tktA* and PB12 *pykAF*$^-$ *ppsA*$^-$ *tyrR*$^-$ *pheA*$^{ev2+}$/pJLB*aroG*^{fbr}*tktA* strains two pulses of glucose (4 g/L each) were added to the cultures when glucose was below 0.5 g/L. In the case of PB12 *pykAF*$^-$ *ppsA*$^-$ *tyrR*$^-$ *pheA*$^{ev2+}$/pJLB*aroG*^{fbr}*tktA*, also one pulse of acetate (at about the same concentration [2 g/L] of its consumption during the first pulse of glucose) was supplemented. For the transcriptional induction of *aroG*^{fbr} and *pheA*^{ev2}, 0.1 mM IPTG was added at the beginning of the culture and tetracycline (30 μg/mL) for plasmid maintenance.

Analytical Procedures

Bacterial growth was spectrophotometrically monitored at 600 nm (DU-70, Beckman Instruments, Inc., Fullerton, CA) and converted to dry cell weight (DCW) per liter using a calibration curve: $1\ OD_{600nm} = 0.37\ g_{DCW}/L$ (Hernández-Montalvo et al., 2003).

Glucose and acetate levels were determined by a Waters HPLC system (Waters Millipore Co., Milford, MA) as reported elsewhere (Martínez-Gómez et al., 2012). Standards of the aromatic intermediates 4-hydroxyphenylpyruvate (HPP) and phenylpyruvate (PPY), as well as the aromatic amino acids L-Tyrosine (L-Tyr) and L-phenylalanine (L-Phe) concentrations were analyzed by a 1100 series Agilent HPLC system (Agilent Technologies, Palo Alto, CA) as has been previously published (Martínez-Gómez et al., 2012). With the exception of PPY, all other compounds were detected on the supernatants of our strains. DAHP concentrations were determined using the thiobarbituric assay (Srinivasan and Sprinson, 1959).

RNA Extraction, cDNA Synthesis, and RT-qPCR Analysis

Total RNA was isolated and purified using a modified hot phenol method reported elsewhere (Aguilar et al., 2012; Flores et al., 2005, 2008) and a RevertAid^{TM} H minus First Strand cDNA Synthesis kit was used to synthesize cDNA according to the manufacturer's instructions (Fermentas, Burlington, Canada). For each reaction, approximately 5 μg of RNA and a mixture of 10 pmol/μL of specific DNA reverse primers (b) for each measured gene were used. The nucleotide sequences of these genes have been previously published (Aguilar et al., 2012; Flores et al., 2005, 2008) RT-qPCR was performed with the ABI Prism 7300 Real-Time PCR System (Perkin Elmer/Applied Biosystems, Foster City, CA) using the Maxima^R SYBR Green/ROX qPCR Master Mix (2×) kit (Fermentas LifeSciences) and reaction conditions previously described (Aguilar et al., 2012). For each gene, all experiments were performed in triplicate from two different fermentations, obtaining very similar values (differences <0.3 SD). A non-template control reaction mixture was included for each gene. Standard curves were constructed to evaluate PCR efficiency and all the qPCR assays showed high efficiency of amplification (90–100%), the genes had R^2 values above 0.9976, with slopes between −3.4 and −3.7. All RT-qPCR experiments were compliant with the MIQE (Minimum Information for Publication of Quantitative Real-Time PCR Experiments) guidelines (Bustin et al., 2009).

The quantification technique used to analyze the data was the $2^{-\Delta\Delta C_q}$ method described by Livak and Schmittgen (2001). Data were normalized using the *ihfB* gene as an internal control (details in Supplementary file 3).

Results and Discussion

Simultaneous Inactivation of PTS and the *pykA*, *pykF*, and *ppsA* Genes Eliminates Growth of the PB11 Derivative on Glucose or Acetate

To elucidate the physiological changes that occur in response to the elimination of PEP and PYR interconversion, we designed strains with gene knockout mutations at the PEP–PYR node. The PB11 *pykAF*$^-$ *ppsA*$^-$ strain was unable to grow with either glucose or acetate as a single carbon source (Table II). It appears that when this strain is growing on glucose, carbon flux through the anaplerotic pathway (Ppc) is restricted, and OAA cannot condense with AcCoA. Furthermore, the inability to produce PYR and then AcCoA may explain why this strain cannot grow on glucose. In this sense, the TCA cycle flux should be highly reduced or absent; therefore, the generation of biosynthetic intermediates and redox power appear to be insufficient to support growth of this PB11 quadruple mutant (*ptsHIcrr*$^-$ *pykAF*$^-$ *ppsA*$^-$) with glucose as carbon source.

On the other hand, the PB11 *pykAF*$^-$ *ppsA*$^-$ strain was not able to grow on acetate because it has diminished levels of PEP due to the inactivation of *ppsA*. Under this gluconeogenic condition, PckA is unable to produce enough PEP from OAA to sustain growth.

Coutilization of Glucose and Acetate Enables Growth of the PB11 *pykAF*$^-$ *ppsA*$^-$ Strain

Due to the absence of the EIIA^{Glc} component, which is mainly responsible for catabolite repression, the simultaneous utilization of carbon substrates has been observed in PTS$^-$ strains (Flores et al., 2005; Martínez et al., 2008). We determined that the PB11 *pykAF*$^-$ *ppsA*$^-$ strain was viable when grown in M9 minimal medium supplemented with glucose plus acetate (Fig. 2). The μ of this quadruple mutant diminished by approximately 40% compared with PB11 (Table II). In addition, the PB11 *pykAF*$^-$ *ppsA*$^-$ strain had a 29% lower maximal biomass concentration and $Y_{X/Glc+Ace}$ compared with its parental strain, PB11 (Table II).

Transcriptional Profiles of Relevant Central Carbon Metabolism Genes Between the PB11 and PB11 *pykAF*$^-$ *ppsA*$^-$ Strains Grown During Coutilization of Glucose and Acetate

RT-qPCR was used to examine the gene expression of 73 genes coding for enzymes and regulatory proteins that participate in the gluconeogenesis, glyoxylate shunt, glycolysis, TCA cycle, and pentose phosphate pathways (Table III).

Glycolytic Genes

As shown above, glucose consumption rate during substrate coutilization in the PB11 *pykAF*$^-$ *ppsA*$^-$ strain was lower than in PB11 (Fig. 2). This result correlates with reduced transcriptional levels of glycolytic genes such as *pfkB*, *fbaB*, *gapC-2*, *pgk*, and genes of the PYR dehydrogenase (Pdh) complex (Fig. 4a). The remainder of the glycolytic genes showed similar expression levels as those in the PB11 strain (Table III). It has been reported that partially blocking the conversion of PEP to PYR increases PEP pool in a *pykF*$^-$ mutant (Siddiquee et al., 2004a), which in turn inhibits some glycolytic enzymes (Ogawa et al., 2007). In this sense, PEP accumulation in the PB11 *pykAF*$^-$ *ppsA*$^-$ strain is feasible because PEP is no longer used as a phosphate donor by the PTS system, and the *ppc* transcriptional level was downregulated (−1.7-fold) during growth on glucose plus acetate compared with its parental strain PB11 (Table III).

Gluconeogenic, Glyoxylate Shunt, and TCA Genes

Expression analysis also revealed that genes involved in acetate catabolism such as *actP*, *acs*, the *aceBAK* operon, *glcB*, *sfcA*, *maeB*, and *pckA* were downregulated in the PB11 *pykAF*$^-$ *ppsA*$^-$ strain compared with PB11 (Fig. 4a). The values for the *actP* (−13.6-fold) and *acs* (−8.4-fold) genes were substantially lower in the PB11 *pykAF*$^-$ *ppsA*$^-$ strain (Table III). These two genes are responsible for the first two steps of acetate catabolism (Gimenez et al., 2003). Recently, a study showed

Table II. Kinetic and stoichiometric parameters for the strain PB11, PB12, and their *pykAF*$^-$ *ppsA*$^-$ derivatives grown on minimal medium with glucose, acetate and glucose plus acetate.*

	Glucose	Acetate	Glucose + acetate			
Strain	μ (h^{-1})	μ (h^{-1})	$\mu_{Glc+Ace}$ (h^{-1})	$q_{Glc+Ace}$ (mmol C/g_{DCW} h)	$Y_{X/Glc+Ace}$ (g_{DCW}/mol C)	Maximal biomass (g/L)
PB11	0.13 ± 0.00	0.18 ± 0.00	0.27 ± 0.01	31.24 ± 1.83	9.51 ± 1.12	1.09 ± 0.07
PB11 *pykAF*$^-$ *ppsA*$^-$	ND	ND	0.16 ± 0.00	23.75 ± 2.32	6.79 ± 0.58	0.78 ± 0.08
PB12	0.40 ± 0.02	0.15 ± 0.01	0.41 ± 0.02	43.77 ± 3.29	9.45 ± 0.00	1.11 ± 0.08
PB12 *pykAF*$^-$ *ppsA*$^-$	0.18 ± 0.01	0.15 ± 0.01	0.33 ± 0.02	38.73 ± 0.81	8.57 ± 0.00	0.85 ± 0.08

ND, not detected.

*These data coincided with values obtained from at least three independent cultures, each one with a duplicate. Differences between values in these experiments were <12%.

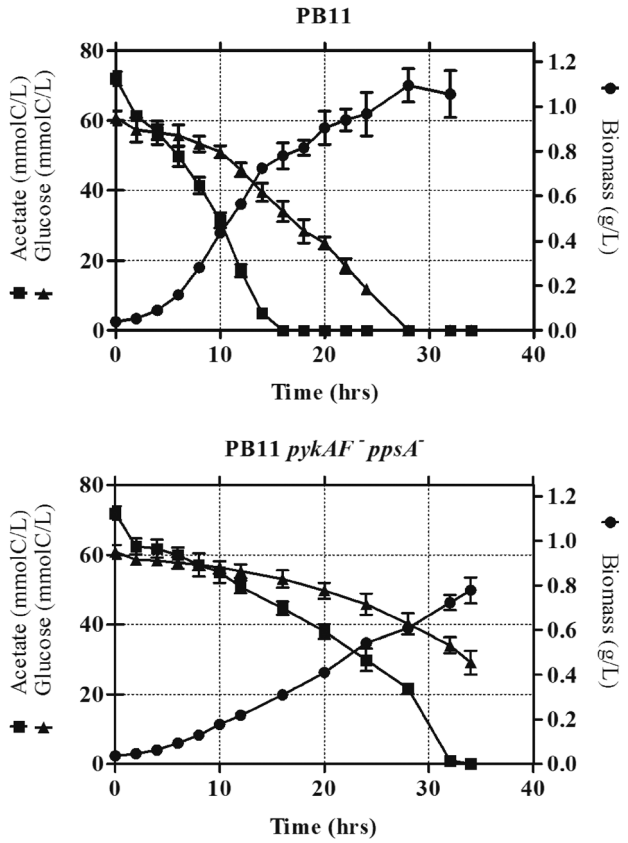

Figure 2. Growth profile and substrate utilization of the PB11 strain and its derivative PB11 *pykAF*$^-$ *ppsA*$^-$. Flask cultures on mineral medium with 2 g/L glucose (equivalent to 67 mmolC/L) and 3 g/L acetate (equivalent to 73 mmolC/L). Differences between values in these experiments were <12%. These data coincided with values obtained from at least three independent cultures, each one with a duplicate.

that when grown on acetate as the only carbon source, the PB11 strain exhibited lower levels of cAMP and lower transcriptional levels of the *actP*, *acs*, *maeB*, and *pckA* genes than its parental strain, JM101 (Sigala et al., 2009). The *acsyjcHactP* and *aceBAK* operons are activated by the cAMP receptor protein (CRP)–cAMP complex; additionally, transcription of the former operon occurs from the *acsP2* promoter, which is dependent on CRP (Wolfe, 2005). The RT-qPCR analysis performed during coutilization of glucose and acetate showed that the transcriptional level of *crp* diminished −1.9-fold, whereas *cya*, which encodes adenylate cyclase, exhibited the same expression level in the PB11 quadruple mutant as in its parental strain. In addition, downregulation of most of the TCA cycle genes in the PB11 *pykAF*$^-$ *ppsA*$^-$ strain compared with those in PB11 (Table III) may also reflect a response to low expression levels of *crp*, gluconeogenic and glyoxylate shunt genes. Taken together, these results reflect a diminished acetate catabolism as a consequence of the simultaneous inactivation of both the *ptsHIcrr* operon and the *pykA*, *pykF*, and *ppsA* genes in the PB11 strain (Fig. 2).

Simultaneous Inactivation of the *pykA*, *pykF*, and *ppsA* Genes Does Not Eliminate Growth of the PB12 Derivative on Glucose or Acetate

In contrast to PB11, the PB12 strain shows a higher glucose transport by an increased level of GalP due to the inactivation of *galR* (Flores et al., 2002, 2005). In addition, the absence of RppH in the PB12 strain causes higher mRNA levels compared with those in the JM101 strain, resulting in enhanced glycolytic and TCA fluxes (Aguilar et al., 2012). The higher glucose consumption capacity of the PB12 strain may explain why the simultaneous inactivation of the *pykA*, *pykF*, and *ppsA* genes did not impair growth of the PB12 derivative on glucose as a sole carbon source. The carboxylation of PEP to oxaloacetate by Ppc is necessary to grow on glucose. The glyoxylate shunt and the malic enzymes appear to be relevant in this quadruple mutant to produce PYR, which cannot be supplied through the normal PEP to PYR route. The PoxB-AckA-Pta-Acs shortcut then appears to be generating the required AcCoA in the PB12 *pykAF*$^-$ *ppsA*$^-$ strain (Fig. 1a). This assumption is consistent with previous reports showing that the disruption of *pykF* or both *pykA* and *pykF* in *E. coli* wild type strains increases the flux through Ppc and the malic enzymes to supply PYR during growth on glucose as the only carbon source (Emmerling et al., 2002; Siddiquee et al., 2004a,b); this could be the case for PB12, but not for the PB11 strain.

On the other hand, when acetate was used as the only carbon source, the inactivation of both Pyks and PpsA in PB12 did not change the μ compared with its parental PB12 strain (Table II). In this case, PEP is no longer produced from PYR and must be synthesized from OAA by PckA. The results on single substrates indicated that in the strain PB12 *pykAF*$^-$ *ppsA*$^-$, the reactions connecting glycolysis and the TCA cycle, such as Ppc and PckA (Fig. 1a), are still active during growth on glucose and acetate, respectively.

Coutilization of Glucose and Acetate Increases Growth in the PB12 *pykAF*$^-$ *ppsA*$^-$ Strain

Simultaneous utilization of both carbon sources significantly increased growth in the PB12 *pykAF*$^-$ *ppsA*$^-$ strain compared with its growth on single substrates. Moreover, glucose and acetate coutilization allowed PB12 *pykAF*$^-$ *ppsA*$^-$ to achieve 80% of the growth rate of PB12 (Table II). Regarding its consumption profile, the former strain exhausted glucose only 4 h after complete depletion in its parental strain and also showed a rapid glucose over acetate consumption, similar to PB12 (Fig. 3). Nevertheless, acetate consumption in the PB12 *pykAF*$^-$ *ppsA*$^-$ strain became slower after glucose depletion. In summary, the simultaneous inactivation of the *pykA*, *pykF*, and *ppsA* genes in PB12 did not affect substantially either the μ or the $q_{Glc+Ace}$ compared with PB12.

Transcriptional Profiles of Relevant Central Carbon Metabolism Genes Between the PB12 and PB12 *pykAF*$^-$ *ppsA*$^-$ Strains Grown During Coutilization of Glucose and Acetate

Expression levels measured by RT-qPCR revealed that values of most of the analyzed genes in PB12 *pykAF*$^-$ *ppsA*$^-$ did not

Table III. Relative transcriptional levels determined by RT-qPCR of several group of genes from the PB11 *pykAF*$^-$ *ppsA*$^-$ and PB12 *pykAF*$^-$ *ppsA*$^-$ strains grown on glucose plus acetate as carbon sources.*

Genes	PB11 *pykAF*$^-$ *ppsA*$^-$	PB12 *pykAF*$^-$ *ppsA*$^-$	Genes	PB11 *pykAF*$^-$ *ppsA*$^-$	PB12 *pykAF*$^-$ *ppsA*$^-$
Gluconeogenesis and glyoxylate shunt			Pentose phosphate pathway		
aceA	−3.89 ± 0.04	4.45 ± 0.37	gnd	−2.53 ± 0.47	0.97 ± 0.08
aceB	−1.86 ± 0.26	5.00 ± 0.24	pgl	−2.48 ± 0.12	1.06 ± 0.28
aceK	−4.15 ± 0.18	4.73 ± 1.04	rpe	−1.74 ± 0.03	0.92 ± 0.08
acs	−8.38 ± 0.04	1.02 ± 0.08	rpiA	0.78 ± 0.03	0.94 ± 0.09
actP	−13.58 ± 0.86	0.81 ± 0.05	rpiB	0.72 ± 0.05	1.26 ± 0.08
fbp	1.07 ± 0.02	0.94 ± 0.20	talA	0.83 ± 0.07	2.09 ± 0.38
glcB	−5.54 ± 0.67	3.10 ± 0.40	talB	−1.84 ± 0.19	1.32 ± 0.15
maeB	−4.00 ± 0.32	1.15 ± 0.13	tktA	0.86 ± 0.04	1.40 ± 0.38
pckA	−3.74 ± 0.05	1.06 ± 0.04	tktB	1.01 ± 0.12	1.50 ± 0.17
sfcA	−1.87 ± 0.04	1.86 ± 0.28	zwf	1.26 ± 0.06	1.24 ± 0.23
Glycolysis			Genes coding for regulatory proteins		
aceE	−1.73 ± 0.09	−2.40 ± 0.05	arcA	−1.61 ± 0.13	1.33 ± 0.33
aceF	−2.14 ± 0.02	−1.60 ± 0.09	arcB	N.D.	1.02 ± 0.10
fbaA	0.69 ± 0.13	1.20 ± 0.11	crp	−1.92 ± 0.11	0.93 ± 0.17
fbaB	−1.92 ± 0.05	1.41 ± 0.18	csrA	−1.85 ± 0.12	0.94 ± 0.12
gapA	−3.17 ± 0.25	1.95 ± 0.37	cyaA	0.87 ± 0.11	1.18 ± 0.10
gapC-1	0.76 ± 0.07	1.04 ± 0.06	fadR	1.30 ± 0.20	0.71 ± 0.10
gapC-2	−1.93 ± 0.32	1.29 ± 0.17	fis	1.15 ± 0.02	1.70 ± 0.32
eno	0.76 ± 0.02	1.55 ± 0.10	fruR	0.74 ± 0.09	1.58 ± 0.29
glk	0.99 ± 0.06	0.99 ± 0.08	iclR	0.71 ± 0.06	1.00 ± 0.14
gpmA	1.22 ± 0.21	1.18 ± 0.15	ihfB	1.00 ± 0.00	1.00 ± 0.00
gpmB	1.14 ± 0.18	1.14 ± 0.20	mlc	0.64 ± 0.02	1.26 ± 0.27
pfkA	1.43 ± 0.18	1.33 ± 0.10	rpoD	1.23 ± 0.03	1.19 ± 0.13
pfkB	−2.08 ± 0.13	2.03 ± 0.09	rpoS	0.98 ± 0.12	1.21 ± 0.11
pgi	1.14 ± 0.07	1.37 ± 0.18	Others		
pgk	−1.77 ± 0.27	2.06 ± 0.34	ackA	0.71 ± 0.01	0.69 ± 0.03
tpi	0.91 ± 0.18	0.94 ± 0.09	galP	1.41 ± 0.37	1.00 ± 0.09
TCA			lamB	−52.89 ± 3.28	1.90 ± 0.55
acnB	−9.52 ± 0.76	1.06 ± 0.11	mglB	−21.44 ± 3.11	0.94 ± 0.08
fumA	−3.66 ± 0.55	1.04 ± 0.04	poxB	0.93 ± 0.00	2.16 ± 0.11
fumB	1.24 ± 0.38	2.75 ± 0.37	ppc	−1.68 ± 0.00	1.34 ± 0.31
fumC	2.12 ± 0.07	2.2 ± 0.27	pta	−1.76 ± 0.09	0.91 ± 0.07
gltA	−4.33 ± 0.00	0.93 ± 0.08	ptsG	−3.37 ± 0.53	0.75 ± 0.04
icdA	−2.86 ± 0.00	1.23 ± 0.10			
lpd	−2.4 ± 0.22	0.94 ± 0.06			
mdh	−3.82 ± 0.17	1.23 ± 0.09			
sdhA	−2.57 ± 0.44	0.98 ± 0.01			
sdhB	−2.61 ± 0.43	0.84 ± 0.13			
sdhC	−1.63 ± 0.18	0.72 ± 0.13			
sdhD	−3.01 ± 0.27	0.81 ± 0.16			
sucA	−2.39 ± 0.32	1.33 ± 0.17			
sucB	−2.38 ± 0.25	1.6 ± 0.36			
sucC	−4.25 ± 0.00	1.14 ± 0.18			
sucD	−3.38 ± 0.05	1.06 ± 0.15			

ND, not determined with adequate SD.

*The transcriptional levels of the measured genes from the control strains (PB11 and PB12, respectively) grown on glucose plus acetate, were considered equal to one and were used as a control to normalize the data. Results presented are the average of three independent measurements of the RT-qPCR expression values for each gene. Values were obtained from different cDNAs generated from three independent bioreactor samples. Expression levels are presented as $2^{-\Delta\Delta C_q}$ (positive values) or $1/2^{-\Delta\Delta C_q}$ (negative values) The RT-qPCR expression values obtained for each gene differ <30%. SD values are shown.

change (56 genes) and others increased (15 genes) compared with the parental PB12 strain. Transcriptional levels of some of these genes are discussed below.

Glycolytic Genes

In PB12 *pykAF*$^-$ *ppsA*$^-$, most of the glycolytic genes maintained the same expression levels as in PB12; only the *pfkB* (2.3-fold), *gapA* (1.95-fold), and *pgk* (2.6-fold) genes were upregulated during coutilization of the substrate mixture (Table III, Fig. 4b). The expression level of *ppc* remained the same in the quadruple mutant compared with its parental strain, which may suggest that in PB12 *pykAF*$^-$ *ppsA*$^-$, Ppc still connects glycolysis and the TCA cycle.

Gluconeogenic, Glyoxylate Shunt, and *poxB* Genes

The expression profile of the PB12 *pykAF*$^-$ *ppsA*$^-$ strain showed that during coutilization of glucose plus acetate, the *aceBAK*, *glcB*, and *scfA* genes were overexpressed compared

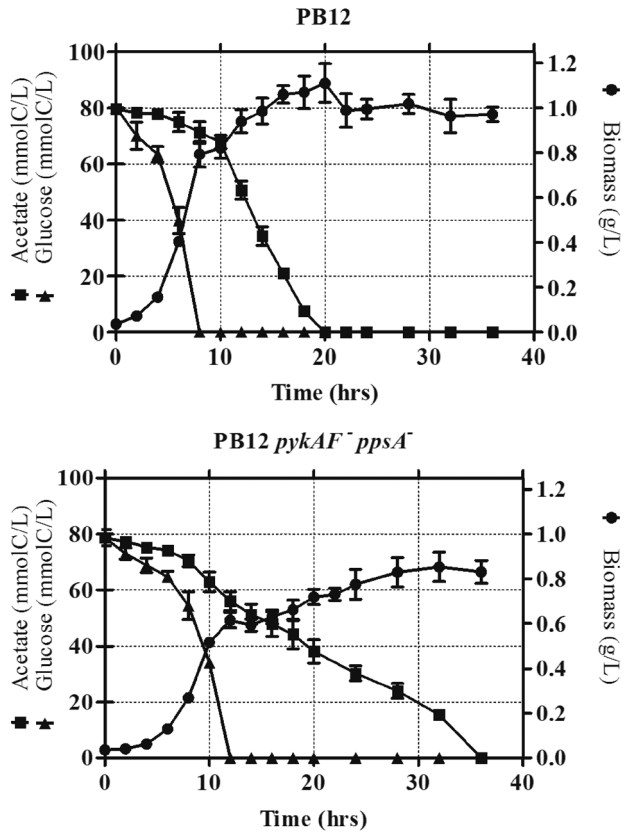

Figure 3. Growth profile and substrate utilization of the PB12 strain and its derivative PB12 *pykAF*$^-$ *ppsA*$^-$. Flask cultures on mineral medium with 2 g/L glucose (equivalent to 67 mmolC/L) and 3 g/L acetate (equivalent to 73 mmolC/L). Differences between values in these experiments were <12%. These data coincided with values obtained from at least three independent cultures, each one with a duplicate.

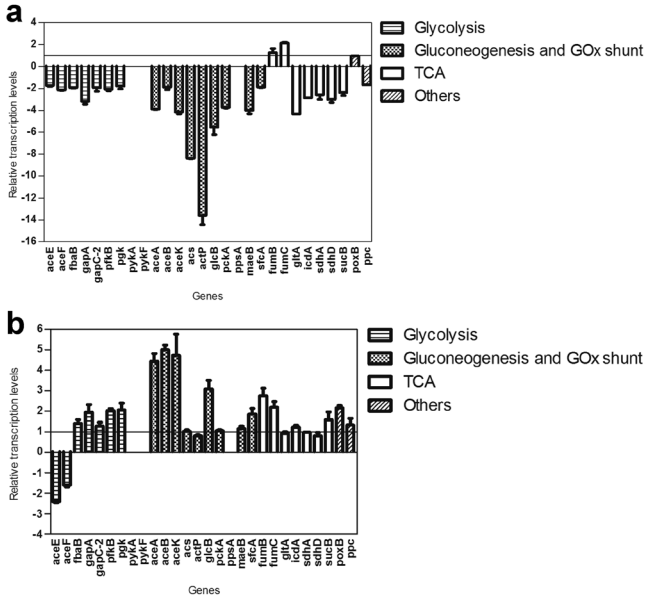

Figure 4. Relative transcriptional levels determined by RT-qPCR for main central carbon metabolism genes. (**a**) PB11 *pykAF*$^-$ *ppsA*$^-$ strain, (**b**) PB12 *pykAF*$^-$ *ppsA*$^-$ strain. The PB11 and PB12 (control strains) RT-qPCR values for the measured genes were set as one. For more details see Table III.

with those in PB12 (Fig. 4b). It is already known that in the evolved PB12 strain, the transcriptional level of the *aceBAK* operon is higher compared with JM101 when glucose is used as carbon source (Flores et al., 2005). It was proposed that acetate produced by PoxB (whose coding gene *poxB* was upregulated) acts as an autoinducer of *aceBAK* by inactivating the isocitrate lyase regulator (IclR). In this study, *poxB* was upregulated twofold in the PB12 *pykAF*$^-$ *ppsA*$^-$ strain when grown on glucose plus acetate (Table III). Under this scenario, acetate partially inactivates the IclR repressor, resulting in the potential derepression of the *aceBAK* operon. Furthermore, results suggested that AcCoA in PB12 *pykAF*$^-$ *ppsA*$^-$ is predominantly formed by the activation of acetate and, to a lesser extent, by the Pdh complex whose coding genes were downregulated in relation to those in its parental strain (Fig. 4b). In addition, the expression level of the *pckA* gene did not change in the PB12 *pykAF*$^-$ *ppsA*$^-$ strain compared with PB12 during coutilization of glucose and acetate, suggesting a possible interconnection between glycolysis and the TCA cycle in the PB12 quadruple mutant.

Aromatics Production in the *ptsHIcrr*$^-$ *pykAF*$^-$ *ppsA*$^-$ Derivatives on Glucose Plus Acetate

In order to indirectly determine the increase in PEP availability in the *ptsHIcrr*$^-$ *pykAF*$^-$ *ppsA*$^-$ strains, their aromatics production capacity was evaluated. As Table IV shows, the q_{TAC} value in the PB12 *pykAF*$^-$ *ppsA*$^-$ *tyrR*$^-$ *pheA*$^{ev2+}$/pJLB*aroG*^{fbr}*tktA* strain was enhanced eightfold when compared with its control strain and reached the highest aromatic compounds titer (8 g/L). Carbon blockage between PEP and PYR in the PB12 *pykAF*$^-$ *ppsA*$^-$ *tyrR*$^-$ *pheA*$^{ev2+}$/pJLB*aroG*^{fbr}*tktA* derivative caused a fourfold increase in its $Y_{TAC/Glc+Ace}$ compared with the PB12 *tyrR*$^-$ *pheA*$^{ev2+}$/pJLB*aroG*^{fbr}*tktA* strain (Table IV). This value represents 65% of the $^{max}Y_{TAC/Glc+Ace}$ value. Considering the genetic modifications performed (Fig. 1b), the increased production of aromatic compounds in the PB12 *pykAF*$^-$ *ppsA*$^-$ *tyrR*$^-$ *pheA*$^{ev2+}$/pJLB*aroG*^{fbr}*tktA* derivative can be related mainly to an improved availability of PEP produced mostly from glycolysis as shown by its higher q_{Glc} with respect to its control strain (Table IV, Fig. 5). In contrast, in the PB11 *pykAF*$^-$ *ppsA*$^-$ *tyrR*$^-$ *pheA*$^{ev2+}$/pJLB*aroG*^{fbr}*tktA* derivative there was no benefit on aromatics production (Table IV) since this strain reduced its q_{Glc} by 47%, and it could cause lower intracellular PEP concentrations. It has been reported that the parental PB11 strain has a reduced glycolytic flux as part of a carbon limitation response compared with PB12 (Flores et al., 2002, 2005, 2007, 2008). In this study, both PB11 derivatives did not totally consume glucose and preferred acetate over glucose consumption as carbon sources (Fig. 6).

Table IV. Aromatic compounds yields and other important parameters determined for the strains PB11 *tyrR*$^{-}$ *pheA*$^{ev2+}$/pJLB*aroG*^{fbr}*tktA*, PB12 *tyrR*$^{-}$ *pheA*$^{ev2+}$/pJLB*aroG*^{fbr}*tktA*, and their *pykAF*$^{-}$ *ppsA*$^{-}$ *tyrR*$^{-}$ *pheA*$^{ev2+}$/pJLB*aroG*^{fbr}*tktA* derivatives in resting cells grown on minimal medium with glucose plus acetate*

Strain	q_{Glc} (mmol C/g_{DCW} h)	q_{Ace} (mmol C/g_{DCW} h)	$q_{Glc+Ace}$ (mmol C/g_{DCW} h)	TAC (g/L)	q_{TAC} (mmol C/g_{DCW} h)	$Y_{TAC/Glc+Ace}$ (mmol C/mmol C)
PB11 *tyrR*$^{-}$ *pheA*$^{ev2+}$/pJLB*aroG*^{fbr}*tktA*	0.95 ± 0.11	2.21 ± 0.27	3.16 ± 0.38	0.29 ± 0.02	0.74 ± 0.05	0.24 ± 0.02
PB11 *pykAF*$^{-}$ *ppsA*$^{-}$ *tyrR*$^{-}$ *pheA*$^{ev2+}$/pJLB*aroG*^{fbr}*tktA*	0.50 ± 0.04	1.75 ± 0.15	2.25 ± 0.19	0.13 ± 0.01	0.14 ± 0.02	0.06 ± 0.01
PB12 *tyrR*$^{-}$ *pheA*$^{ev2+}$/pJLB*aroG*^{fbr}*tktA*	3.87 ± 0.18	0.95 ± 0.04	4.81 ± 0.22	1.24 ± 0.11	0.59 ± 0.05	0.12 ± 0.01
PB12 *pykAF*$^{-}$ *ppsA*$^{-}$ *tyrR*$^{-}$ *pheA*$^{ev2+}$/ pJLB*aroG*^{fbr}*tktA*	5.32 ± 0.12	2.11 ± 0.05	7.41 ± 0.17	8.08 ± 0.47	5.11 ± 0.30	0.52 ± 0.03

TAC, total aromatic compounds (DAHP, HPP, L-Tyr, and L-Phe).

*These data coincided with values obtained from at least three independent cultures, each one with a duplicate. Differences between values in these experiments were <15%.

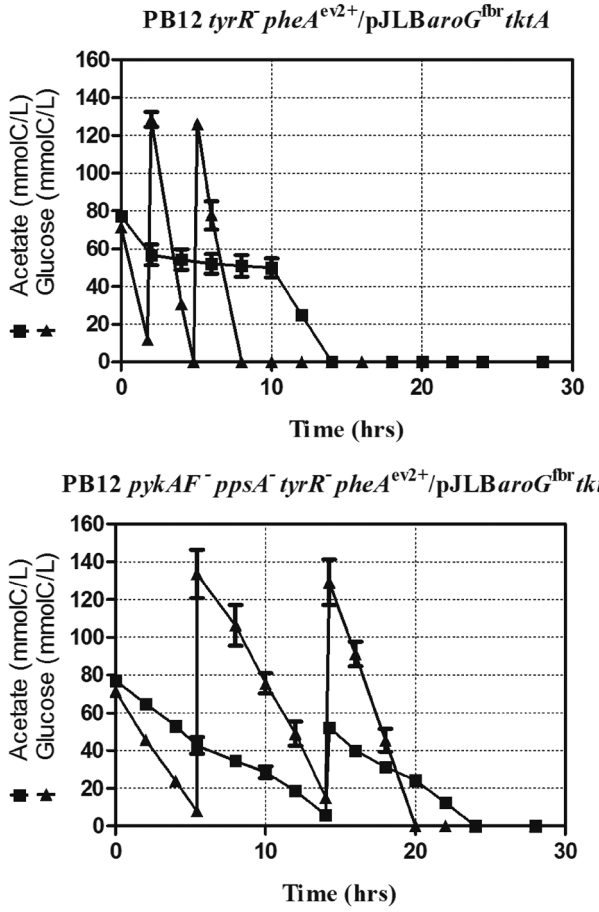

Figure 5. Substrate utilization in resting cells of PB12 *tyrR*$^{-}$ *pheA*$^{ev2+}$/pJLB*aroG*^{fbr}*tktA* strain and its derivative PB12 *pykAF*$^{-}$ *ppsA*$^{-}$ *tyrR*$^{-}$ *pheA*$^{ev2+}$/pJLB*aroG*^{fbr}*tktA*. Flask cultures on mineral medium with 2 g/L glucose and 3 g/L acetate. Differences between values in these experiments were <15%. These data coincided with values obtained from at least three independent cultures, each one with a duplicate. The biomass value for the first strain was 2.54 ± 0.12, whereas for the second one was 1.83 ± 0.04 (data not shown).

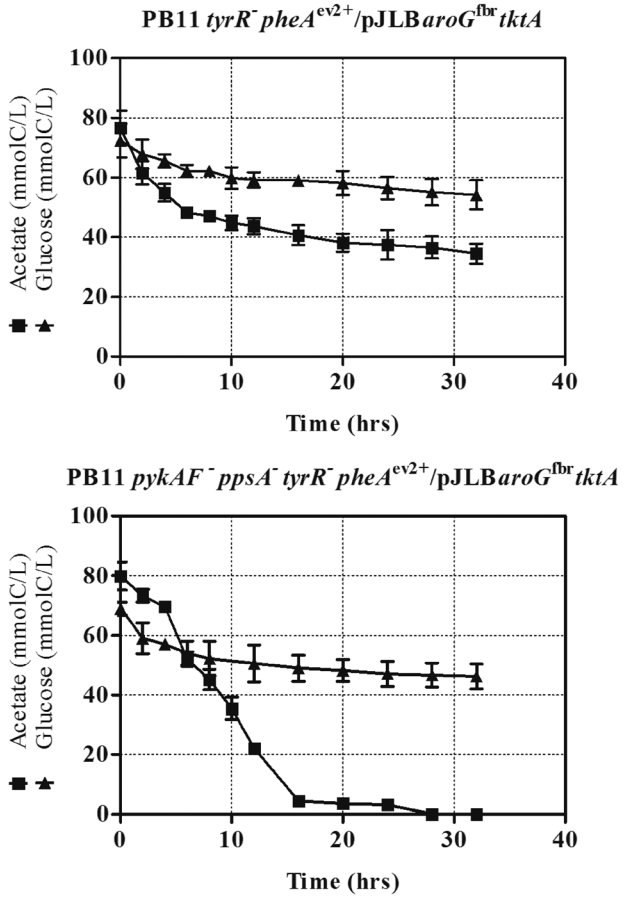

Figure 6. Substrate utilization in resting cells of PB11 *tyrR*$^{-}$ *pheA*$^{ev2+}$/pJLB*aroG*^{fbr}*tktA* strain and its derivative PB11 *pykAF*$^{-}$ *ppsA*$^{-}$ *tyrR*$^{-}$ *pheA*$^{ev2+}$/pJLB*aroG*^{fbr}*tktA*. Flask cultures on mineral medium with 2 g/L glucose and 3 g/L acetate. Differences between values in these experiments were <15%. These data coincided with values obtained from at least three independent cultures, each one with a duplicate. The biomass value for the first strain was 0.60 ± 0.07, whereas for the second one was 1.44 ± 0.13 (data not shown).

In fact, acetate was completely exhausted in the PB11 *pykAF*$^-$ *ppsA*$^-$ *tyrR*$^-$ *pheA*$^{ev2+}$/pJLB*aroG*^{fbr}*tktA* derivative compared with its control strain. Besides, glucose contribution to aromatic compounds production (1 mol Glc → 0.58 mol TAC) is higher compared with acetate catabolism (1 mol Ace → 0.22 mol TAC). Therefore acetate consumption by itself in the PB11 *pykAF*$^-$ *ppsA*$^-$ *tyrR*$^-$ *pheA*$^{ev2+}$/pJLB*aroG*^{fbr}*tktA* derivative is not enough to increase significantly carbon flow from the TCA cycle towards the aromatic biosynthetic pathway.

Conclusions

We described features of the physiology of *ptsHIcrr*$^-$ derivatives during simultaneous utilization of glucose and acetate and provided information regarding their metabolic plasticity when the PEP and PYR interconversion is blocked by deleting the *pykA*, *pykF*, and *ppsA* genes. We have shown that in the PB11 *pykAF*$^-$ *ppsA*$^-$ strain there is a separation of glycolysis and the TCA cycle because no growth was detected on single glucose or acetate substrates. Interestingly, this quadruple mutant is viable when coutilizing glucose and acetate. Under this condition, the *ppc* and *pckA* genes (whose enzymes connect glycolysis and the TCA cycle) were downregulated relative to those in its parental strain. Taking these results together, glycolysis and the TCA cycle appear to coexist independently in the PB11 *pykAF*$^-$ *ppsA*$^-$ strain during simultaneous utilization of glucose and acetate as carbon sources. However, the PB11 *pykAF*$^-$ *ppsA*$^-$ strain had a lower μ and $q_{Glc+Ace}$ than PB11. In agreement with this result, genes involved in the transport and consumption of acetate (*acs*, *actP*, and *aceBAK* operon) as well as some glycolytic genes (*fbaB*, *gapA*, *gapC-2*, *pgk*, and *pfkB*) were downregulated in the quadruple mutant compared with those in PB11. In contrast, a partial separation of glycolysis and the TCA cycle was achieved in the PB12 *pykAF*$^-$ *ppsA*$^-$ derivative because this strain can grow on glucose or acetate. Coutilization of glucose and acetate in this evolved *ptsHIcrr*$^-$ *pykAF*$^-$ *ppsA*$^-$ strain maintained its μ and $q_{Glc+Ace}$ at 80% and 88%, respectively, compared with PB12. The RT-qPCR analysis showed that when coutilizing substrates, the PB12 *pykAF*$^-$ *ppsA*$^-$ strain upregulates the *aceBAK* operon and the *sfcA* gene. In addition, the engineered PB12 *pykAF*$^-$ *ppsA*$^-$ *tyrR*$^-$ *pheA*$^{ev2+}$/pJLB*aroG*^{fbr}*tktA* derivative achieved a fourfold higher $Y_{TAC/Glc+Ace}$ compared with its control strain, representing 65% of the $^{max}Y_{TAC/Glc+Ace.}$

The authors also thank Larisa Cortés, Mercedes Enzaldo, and Ramón de Anda for their technical support.

References

Aguilar C, Escalante A, Flores N, de Anda R, Riveros-McKay F, Gosset G, Morett E, Bolívar F. 2012. Genetic changes during a laboratory adaptive evolution process that allowed fast growth in glucose to an *Escherichia coli* strain lacking the major glucose transport system. BMC Genomics 13:385.

Báez-Viveros JL, Osuna J, Hernández-Chávez G, Soberón X, Bolívar F, Gosset G. 2004. Metabolic engineering and protein directed evolution increase the yield of L-phenylalanine synthesized from glucose in *Escherichia coli*. Biotechnol Bioeng 87:516–524.

Balderas-Hernández VE, Sabido-Ramos A, Silva P, Cabrera-Valladares N, Hernández-Chávez G, Báez-Viveros JL, Martínez A, Bolívar F, Gosset G. 2009. Metabolic engineering for improving anthranilate synthesis from glucose in *Escherichia coli*. Microb Cell Fact 8:19.

Bustin SA, Benes V, Garson JA, Hellemans J, Huggett J, Kubista M, Mueller R, Nolan T, Pfaffl MW, Shipley GL, Vandesompele J, Wittwer CT. 2009. The MIQE guidelines: Minimum information for publication of quantitative real-time PCR experiments. Clin Chem 55:611–622.

Covert MW, Palsson BØ. 2002. Transcription regulation in constraints-based metabolic models of *Escherichia coli*. J Biol Chem 277:28058–28064.

Datsenko KA, Wanner BL. 2000. One step inactivation of chromosomal genes in *Escherichia coli* K-12 using PCR products. Proc Natl Acad Sci USA 97:6640–6645.

Emmerling M, Dauner M, Ponti A, Fiaux J, Hochuli M, Szyperski T, Wüthrich K, Bailey JE, Sauer U. 2002. Metabolic flux responses to pyruvate kinase knockout in *Escherichia coli*. J Bacteriol 184:152–164.

Escalante A, Calderón R, Valdivia A, de Anda R, Hernández G, Ramírez OT, Gosset G, Bolívar F. 2010. Metabolic engineering for the production of shikimic acid in an evolved *Escherichia coli* strain lacking the phosphoenolpyruvate: Carbohydrate phosphotransferase system. Microb Cell Fact 9:21.

Fischer E, Sauer U. 2003. Metabolic flux profiling of *Escherichia coli* mutants in central carbon metabolism using GC–MS. Eur J Biochem 270:880–891.

Flores N, Xiao J, Berry A, Bolívar F, Valle F. 1996. Pathway engineering for the production of aromatic compounds in *Escherichia coli*. Nat Biotechnol 14:620–623.

Flores N, Flores S, Escalante A, de Anda R, Leal L, Malpica R, Georgellis D, Gosset G, Bolívar F. 2005. Adaptation for fast growth on glucose by differential expression of central carbon metabolism and *gal* regulon genes in an *Escherichia coli* strain lacking the phosphoenolpyruvate: Carbohydrate phosphotransferase system. Metab Eng 7:70–87.

Flores N, Leal L, Sigala JC, de Anda R, Escalante A, Martínez A, Ramírez OT, Gosset G, Bolívar F. 2007. Growth recovery on glucose under aerobic conditions of an *Escherichia coli* strain carrying a phosphoenolpyruvate: Carbohydrate phosphotransferase system deletion by inactivating *arcA* and overexpressing the genes coding for glucokinase and galactose permease. J Mol Microbiol Biotechnol 13:105–116.

Flores N, Escalante A, de Anda R, Báez-Viveros JL, Merino E, Franco B, Georgellis D, Gosset G, Bolívar F. 2008. New insights into the role of sigma factor RpoS as revealed in *Escherichia coli* strains lacking the phosphoenolpyruvate: Carbohydrate phosphotransferase system. J Mol Microbiol Biotechnol 14:176–192.

Flores S, Gosset G, Flores N, de Graaf AA, Bolívar F. 2002. Analysis of carbon metabolism in *Escherichia coli* strains with an inactive phosphotransferase system by ^{13}C labeling and NMR spectroscopy. Metab Eng 4:124–137.

Gimenez R, Nuñez MF, Badia J, Aguilar J, Baldosa L. 2003. The gene *yjcG*, cotranscribed with gene *acs*, encodes an acetate permease in *Escherichia coli*. J Bacteriol 185:6448–6455.

Hernández-Montalvo V, Martínez A, Hernández-Chávez G, Bolívar F, Valle F, Gosset G. 2003. Expression of *galP* and *glk* in a *Escherichia coli* PTS mutant restores glucose transport and increases glycolytic flux to fermentation products. Biotechnol Bioeng 83:687–694.

Holms WH. 1986. The central metabolic pathways of *Escherichia coli*: Relationship between flux and control at a branch point, efficiency of conversion to biomass, and excretion of acetate. Curr Top Cell Regul 28:69–105.

Livak KJ, Schmittgen TD. 2001. Analysis of relative gene expression data using real-time quantitative PCR and the $2^{-\Delta\Delta CT}$ method. Methods 25:402–408.

Martínez K, de Anda R, Hernández G, Escalante A, Gosset G, Ramírez OT, Bolívar F. 2008. Coutilization of glucose and glycerol enhances the production of aromatic compounds in an *Escherichia coli* strain lacking the phosphoenolpyruvate: Carbohydrate phosphotransferase system. Microb Cell Fact 7:1.

Martínez-Gómez K, Flores N, Castañeda HM, Martínez-Batallar G, Hernández-Chávez G, Ramírez OT, Gosset G, Encarnación S, Bolívar

F. 2012. New insights into *Escherichia coli* metabolism: Carbon scavenging, acetate metabolism and carbon recycling responses during growth on glycerol. Microb Cell Fact 11:46.

Messing J. 1979. A multipurpose cloning system based on the single stranded DNA bacteriophage M13. Recomb DNA Tech Bull 2:43–48.

Meza E, Becker J, Bolívar F, Gosset G, Wittmann C. 2012. Consequences of phosphoenolpyruvate:sugar phosphotransferase system and pyruvate kinase isozymes inactivation in central carbon metabolism flux distribution in *Escherichia coli*. Microb Cell Fact 11:127.

Ogawa T, Mori H, Tomita M, Yoshino M. 2007. Inhibitory effect of phosphoenolpyruvate on gycolytic enzymes in *Escherichia coli*. Res Microbiol 158:159–163.

Oh MK, Rohlin L, Kao KC, Liao JC. 2002. Global expression profiling of acetate-grown *Escherichia coli*. J Biol Chem 277:13175–13183.

Palmeros B, Wild J, Szybalski W, Le Borgne S, Hernández-Chávez G, Gosset G, Valle F, Bolívar F. 2000. A family of removable cassettes designed to obtain antibiotic-resistance free genomic modifications of *Escherichia coli* and other bacteria. Gene 247:255–264.

Postma PW, Lengeler JW, Jacobson GR. 1996. Phosphoenolpyruvate: Carbohydrate phosphotransferase systems. In: Neidhart FC, editor. *Escherichia coli* and *Salmonella*. Cellular and molecular biology. Washington, D.C.: ASM Press. p 1149–1179.

Sabido A, Martínez LM, de Anda R, Martínez A, Bolívar F, Gosset G. 2013. A novel plasmid vector designed for chromosomal gene integration and expression: Use for developing a genetically stable *Escherichia coli* melanin production strain. Plasmid 69:16–23.

Sauer W, Eikmanns BJ. 2005. The PEP–pyruvate–oxaloacetate node as the switch point for carbon flux distribution in bacteria. FEMS Microbiol Rev 29:765–794.

Siddiquee KAZ, Arauzo-Bravo MJ, Shimizu K. 2004a. Metabolic flux analysis of *pykF* gene knockout *Escherichia coli* based on ^{13}C-labelling experiments together with measurements of enzyme activities and intracellular metabolite concentrations. Appl Microbiol Biotechnol 63:407–417.

Siddiquee KAZ, Arauzo-Bravo MJ, Shimizu K. 2004b. Effect of a pyruvate kinase (*pykF*-gene) knockout mutation on the control of gene expression and metabolic fluxes in *Escherichia coli*. FEMS Microbiol Lett 235: 25–33.

Sigala JC, Flores S, Flores N, Aguilar C, de Anda R, Gosset G, Bolívar F. 2009. Acetate metabolism in *Escherichia coli* strains lacking phosphotransferase system; evidence of carbon recycling strategies and futile cycles. J Mol Microbiol Biotechnol 16:224–235.

Srinivasan PR, Sprinson DB. 1959. 2-Keto-3-deoxy-D-arabo-heptonic acid 7-phosphate synthetase. J Biol Chem 234:716–722.

Wolfe AJ. 2005. The acetate switch. Microbiol Mol Biol Rev 69:12–50.

Yang C, Hua Q, Baba T, Mori H, Shimizu K. 2003. Analysis of *Escherichia coli* anaplerotic metabolism and its regulation mechanisms from the metabolic responses to altered dilution rates and phosphoenolpyruvate carboxykinase knockout. Biotechnol Bioeng 84:129–144.